International Journal of Pattern Recognition
and Artificial Intelligence
Vol. 30, No. 7 (2016) 1655018 (25 pages)

DOI: 10.1142/S0218001416550181

World Scientific
www.worldscientific.com

# A Hybrid Skin Detection Model from Multiple Color Spaces Based on a Dual-Threshold Bayesian Algorithm

Fujunku Chen*,‡, Zhigang Hu*, Keqin Li† and
Wei Liu*

*School of Software, Central South University
Changsha, Hunan, P. R. China

†Department of Computer Science, State University of New York
New Paltz, NY 12561, USA
‡kuchen@csu.edu.cn

Received 10 December 2015
Accepted 12 February 2016
Published 29 April 2016

As a preliminary step of many applications, skin detection serves as an irreplaceable role in image processing applications, such as face recognition, gesture recognition, web image filtering, and image retrieval systems. Combining information from multiple color spaces improves the recognition rate and reduces the error rate because the same color is represented differently in other color spaces. Consequently, a hybrid skin detection model from multiple color spaces based on a dual-threshold Bayesian algorithm (DTBA) has been proposed. In each color space, the pixels of images are divided into three categories, namely, skin, nonskin, and undetermined, when using the DTBA. Then, nearly all skin pixels are obtained by using a specific rule that combines the recognition results from multiple color spaces. Furthermore, skin texture filtering and morphological filtering are applied to the results by effectively reducing false identified pixels. In addition, the proposed skin model can overcome interference from a complex background. The method has been validated in a series of experiments using the Compaq and the high-resolution image datasets (HRIDs). The findings have demonstrated the proposed approach produced an improvement, the true positive rate (TPR) improves more than 6% and the false positive rate (FPR) reduces more than 11%, compared with the Bayesian classifier. We confirm that the method is competitive. Meanwhile, this model is robust against skin distribution, scaling, partial occlusions, and illumination variations.

*Keywords*: Dual-threshold Bayesian algorithm; hybrid skin model; image process; multiple color spaces; skin detection; skin segmentation.

## 1. Introduction

Skin detection is the process of selecting human skin regions from an image. Recently, skin detection has been widely applied, especially with the widespread use of

‡Corresponding author.

video capture devices and the popularity of smartphones. In short, skin detection facilitates plenty of applications. In regard to biometric identification technology, human biological characteristics are used for identity authentication of which the representative examples include face recognition, fingerprint recognition, and palm print recognition. In an image retrieval system, skin detection is used for pornographic image filtering,[34,35] photo beautification and the automatic classification of images. Additionally, it has been successfully applied to the analysis of video surveillance, cosmetic effects, human-computer interaction, and the analysis of the polygraph based on behaviors. To be more specific, Song has presented a new feature descriptor named multi-scale histograms of principal oriented gradients by combining multiple feature sets that describe the characteristics of eyes to determine whether the eyes are closed.[2,5] As the first step of face recognition, skin detection has the ability to narrow the search area effectively and reduce the amount of computation greatly.[2] Thanks to the utilization of skin detection, the accuracy of the face recognition system has been improved.[33] However, most of the studies are focused on image recognition in the visible spectrum, which is affected by various factors including light intensity, the characteristics of the camera, and the ethnicity of the person. These factors cause difficulty when performing the research.[14]

Skin detection methods can be divided into two types: statistical methods and physical process methods. Statistical methods consist of two processes, namely, color space selection and skin modeling, which can be subdivided into three types: the parametric model, the nonparametric model and the semi-parametric model. The parametric model is expressed by explicit functions, while the nonparametric model is not fixed. The semi-parametric model, which uses the same parameters by adjusting to optimize the outcome, generally refers to a neural network. Nevertheless, through the combination of spectral characteristics and the skin color reflection model, methods based on a physical imaging process study the influence of light. In general, as the skin detection algorithm is used diffusely, there are very successful products in different fields.

Photo beautification applications prevail, especially for those applications that include humans. People always focus on the face and skin when modifying a photo, and the skin detection method matters. For the sake of more highly valued photos, obtaining whole skin pixels with few misclassified pixels becomes more important. In this paper, the hybrid skin detection model is proposed for detecting all skin pixels under an intricate background with similar skin pixels. The main idea of the hybrid skin detection model is using the joint probability to induce the error rate and increase the recognition rate because the same color is represented differently in other color spaces. At the same time, the double-threshold Bayesian algorithm contributes to the precision in which the pixels are classified into three categories, namely, skin, nonskin, and undetermined. First, the novel double-threshold Bayesian method is used to separate pixels into three categories from each and every color space, where the double thresholds are gained from the training set. Then, the pixels are extracted

by combining the identified results from multiple color spaces using a discriminant. Finally, the recognition results are refined by a skin texture filter and a morphological filter.

The rest of this paper is organized as follows: Section 2 describes the achievements in skin detection. Section 3 introduces the construction of the naïve Bayesian classifier. The hybrid skin detection model we proposed is discussed in Sec. 4. The results of the hybrid model are evaluated and compared in Sec. 5, where several experimental images are shown. In Sec. 6, the conclusion is given.

## 2. Literature Review

In general, one of the most commonly used methods for skin detection is the provision of skin color, which utilizes an expression to define the range of color. To illustrate, in color space YCbCr, the CbCr plane is employed to determine the skin pixels regardless of the lightness component (Y).[6] After that, a variety of color spaces with prescribed ranges have been proposed.

Admittedly, the Bayesian method is extensively applied in statistical models. Proposed by Michael,[13] the statistical color model considers not only the skin color but also the nonskin color. Different color spaces that use the Bayesian method have come forth: YCbCr, HSV, and nRGB. Moreover, in the intuitive color space, which is obtained by using the nonlinear change of RGB, is composed of hue, saturation, and intensity. This color space was used by Garicia for skin detection.[11] To achieve a detection result rapidly in a real-time system, an approach without color space transformation was proposed by Chen.[7] Then, the regular three-dimensional (3D) color spaces and two-dimensional (2D) chrominance planes were reviewed by adopting the cohesiveness and separability of skin color that evaluated the performance of the classifiers.[24] The conclusion showed that RGB was the optimal 3D color space. Meanwhile, wiping the luminance information would reduce the separability. The existing skin detection methods were discussed by Shoyaib, including the color spaces, image datasets, true positive rate (TPR), and false positive rate (FPR).[23] Recently, studies on skin detection by Tsitsoulis combined a global detection technology with an appearance model that used the r, g, s, I, a, and Cr channels.[28] For the purpose of obtaining an accurate result, the machine learning method was proposed to construct an optimal color space that can be partitioned by a simple rule.

The neural network, which is one of the most state-of-the-art skin detection methods, is considered as the most suitable approach for skin detection in semiparametric.[8] Based on skin color likelihood, Yuseok used the Boosting algorithm to enhance skin color information and made a dent in the nonskin information at the same time.[1] Similarly, Michael used texture and spatial features to intensify the separability of skin color. Duan proposed a neural network method based on pulse couple to identify human skin areas.[9] Moreover, by adopting a pixel-based classification method, Bhoyar created a novel symmetry neural network classifier in YCbCr.[3] Chemical reaction optimization has showed significant performance in

neural network training,[17] A double molecular structure-based chemical reaction optimization (DMSCRO) method is developed to improve the result,[31] and it can be applied to image processing. In RGB, the partial color invariance algorithm was tested in a complex light environment. However, some similar skin colors were classified incorrectly. The traditional neural network algorithms were complex and computationally time consuming. An automatic segmentation approach based on self-generating neural network (SGNN) and genetic algorithm (GA) was proposed. A seed, which was selected by using GA, was used to initialize a neural tree. Then, the neural forest was generated by SGNN.[30] The clustering model, introduced by Sinan, partitioned the skin by extending the marked seed pixels.[18] Nevertheless, the parametric model paid more attention to reach the target in the case of limited training samples. For example, take the single gaussian model (SGM) and gaussian mixture model (GMM). It works well by using interpolation with litter samples. In addition, a small quantity of parameters and a storage space were needed.[29] Compared with the statistical probability model (SPM), it needs more training time.[19] At the same time, only the skin color distribution was considered, which is closely dependent on the samples. In spite of the widely studied statistic models, it also has some shortcomings when considering that the color information at the pixel lever is incomplete, which has caused plenty of incorrect identifications such as animal fur and deserts.

Owing to the limitation of a single model, the hybrid models arose. Juan presented an approach that two detectors were used to obtain a high and low probability for the pixel area. Then, the threshold partition was taken. Finally, the results of the two detectors were combined by morphological reconstruction.[22] By taking into account the skin texture features, the skin likely pixels were filtered. Zaidan used a four-phase anti-pornography based on Bayesian and neural methods, namely, preliminary study phase, modeling phase, development phase, and evaluation phase.[35] Pisharady generated a saliency map by using of Bayesian model to detect the hand region, the model also combined the shape, texture, and color features in hand postures recognition.[21] Duffner used the shape-based upper-body detections to classify the soft segmentation and fused both detection and segmentation score to improve the precision.[10] Naji made use of hue and saturation to establish a multi-layer clustering model of the skin color, and the skin color was extracted by four clustering models. In the end, a color correction algorithm was applied; thus, the experiment reached a high accuracy and a low false recognition rate.[18] Michael proposed a discriminative skin-presence feature space to analyze skin pixels, the method extracts textural features from the skin probability maps rather than the luminance channel. However, the accuracy is depending on the feature selection which is also time consuming.[16] Yogarajah presented a novel online learned dynamic thresholds to overcome the drawbacks of fixed decision boundaries.[32] Kawulok combined an adaptive method with the spatial analysis of skin pixels, where a local dynamic skin model is used to extract seeds for spatial analysis.[15] In order to decrease the number of false

alarms, the authors utilized the Harr-like and AdaBoost techniques to detect face or hand.[5] However, those models heavily depend on the performance of the eyes detection, hand or face detection. In order to overcome the changes in skin color because of tan level, races, genders, and illumination conditions, Bianco built an *ad hoc* skin classifier for each person in an image, and that is computation consuming.[4] In addition, the method adaptively chooses between pixel-based, face-based, and both face-based and body-based skin classifiers. Furthermore, a skin recognition method was performed using the Dempster–Shafer evidence theory in literature.[23] In addition, recognition speed is one of the most important aspects of skin recognition. Sun run is a local skin model for improving the global skin model.[26]

However, several problems must be addressed in the above methods. To illustrate these problems, there is no effective method that can distinguish between the skin and similar colored pixels in complex surroundings exactly, especially in the single color space methods. Some models require a long training time and a large number of parameters for adjustment, such as the neural network method, which needs plenty of arduous work.[23] More importantly, no overall skin pixel segmentation method has been proposed. From this respect, more attention and progress are needed. To gain nearly all of the skin pixels of a photo, a more precious approach is needed. Although there is research regarding skin detection from multiple color spaces, they only use a classifier that divides pixels into two categories in each color space with a classify border that always contains many misclassified pixels. The dual-threshold Bayesian algorithm (DTBA) solves the problem perfectly by defining a range to cover the misclassified pixels, which is labeled as undetermined. Finally, the skin texture filter and morphological filter refine the detected results.

## 3. Related Concepts

Skin detection mainly includes two processes. One process is color space transformation, where the source image is converted to different color spaces. The other process is skin modeling, where a mathematical model is established to fit the color distribution by analyzing the existing data. Afterward, the model is used to predict or detect skin pixels. The selection of the color space affects the performance of color recognition. To obtain the best color space, many analyses and comparisons were performed by researchers. Nevertheless, no consistent agreement was reached. After comparing the performance of two skin detection models in nine different color spaces, Terrillon[27] came to the conclusion that the correlation of components are too high in RGB and that converting to a color space whose luminance and chrominance are separated is helpful. At the pixel level, the luminance contributed to the skin detection. As for how to choose the best color space, there is no conclusion. However, the combination of color spaces can optimize the recognition result.

Statistical probability model makes full use of a statistical histogram for skin detection. Then, a probability lookup table for skin and nonskin is available through SPM. $P(\text{color}|\text{skin})$ and $P(\text{color}|\text{nonskin})$ are the prior probability that stand for the

probability of a skin (or nonskin) pixel in the whole dataset. To classify images, $P(\text{skin}|\text{color})$ and $P(\text{nonskin}|\text{color})$ are more accurate, namely, they are the probability of a specified color that will be skin (or nonskin). The probabilities can be obtained according to Bayesian rule Eq. (1):

$$P(\text{skin}|\text{color}) = \frac{P(\text{color}|\text{skin})P(\text{skin})}{P(\text{color}|\text{skin})P(\text{skin}) + P(\text{color}|\text{nonskin})P(\text{nonskin})}, \quad (1)$$

where $P(\text{color}|\text{skin})$ and $P(\text{color}|\text{nonskin})$ can be achieved by SPM. At the same time, $P(\text{skin})$ and $P(\text{nonskin})$ are fixed for the training set; hence, the rule is simplified as Eq. (2):[13]

$$L(\text{color}) = \frac{P(\text{color}|\text{skin})}{P(\text{color}|\text{nonskin})}, \quad (2)$$

where $L(\text{color})$ indicates the ratio of the probability of a color appearing as skin and nonskin. After that, $L(\text{color})$ is normalized. By selecting the proper classification threshold $\theta$ and comparing it with calculated $L(\text{color})$, the skin areas are gained. The naïve Bayesian method runs fast with an acceptable recognition rate, and it is robust to the posture and position of the human body. Nevertheless, only one color space's information is considered, and the change in illumination has a great influence on the recognition result.

## 4. The Proposed Model

The skin model constructed in this paper is divided into two parts (Fig. 1): one part is the DTBA based on multiple color spaces. The other part is the skin texture and the morphological filter. This paper mainly focuses on the former. In short, the hybrid skin model we proposed takes the sample images labeled with skin, the original images, the TPR and the FPR as input, while the model outputs original images with the skin area labeled. In the training phase, the sample image is converted to different color spaces. Then, SPM is used to obtain the dual-threshold value. In the testing phase, the original images are tested with the hybrid skin detection model.

### 4.1. *DTBA based on multiple color spaces*

In each color space, the recognition results are different. The combination of the recognition results of different color spaces results in a higher recognition rate and a lower false recognition rate.

#### 4.1.1. *Dual-threshold bayesian algorithm*

The DTBA is based on multiple color spaces, whose main process is conducting skin detection in each color space. Then, by combining the recognition results from each color space with a certain rule, the synthesized skin area was achieved and the misclassified pixels were excluded.

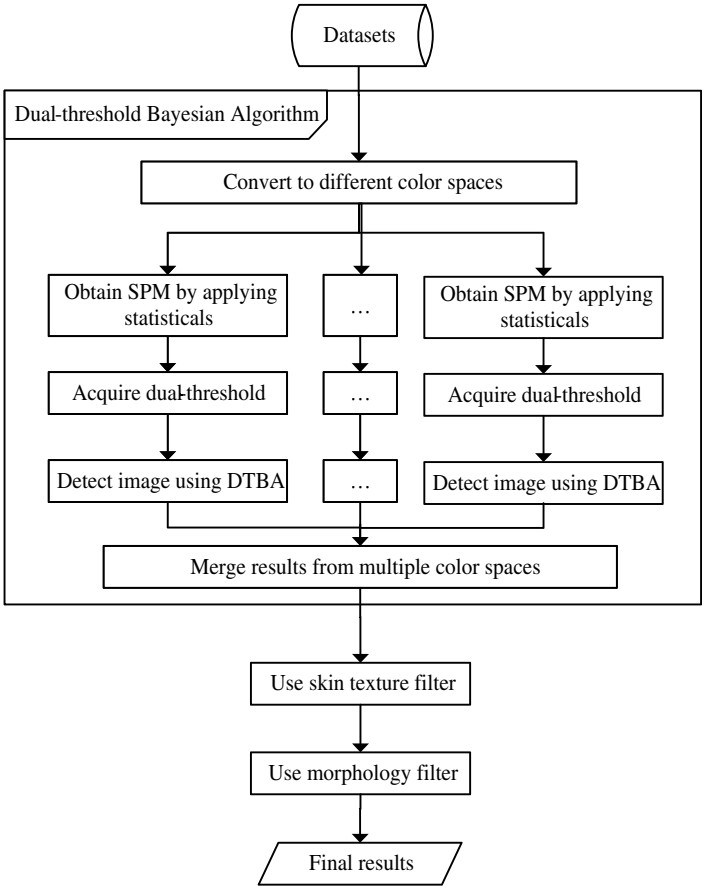


Fig. 1. The main procedures of the proposed model.

In the RGB color space, the TPRs and FPRs of the skin detection model with a variation in the thresholds changes. The threshold ($\theta_1$), when the recognition rate is high, is taken as the lower bound. The threshold ($\theta_2$), when the recognition rate is low, is taken as the upper bound for the classification. As a consequence, the interval 0–1 is divided into three sections by the two thresholds, as shown in Eq. (3). Specifically, $[0, \theta_1)$ contains only a small amount of skin pixels. In $(\theta_2, 1]$, few nonskin pixels are mistaken, while in $[\theta_1, \theta_2]$, additional steps are executed to classify the pixels:

$$g(x,y) = \begin{cases} \text{Skin}, & f(x,y) \le \theta_1 \\ \text{Undetermined}, & \theta_1 < f(x,y) < \theta_2 \\ \text{Nonskin}, & f(x,y) \ge \theta_2 \end{cases}, \tag{3}$$

where $(x, y)$ is the coordinate of an image, which corresponds to a pixel. $f(x, y)$ stands for the ratio of the color's probability as skin and nonskin, while $g(x,y)$ serves

as the classification result of $(x, y)$. $\theta_1$ and $\theta_2$ stand for the lower and upper bounds, respectively.

#### 4.1.2. *The principle of using multiple color spaces*

Previous studies show that the recognition rate and performance vary from one color space to another. However, there are few investigations regarding the relationship of the recognition results detected by the same skin model in different color spaces. In this paper, we proposed to use the Bayesian classification algorithm for skin detection in each color space. Then, we combine the result with intersection and union operations. After that, the TPRs and FPRs of the color space combinations were obtained, which are the metrics for the color space combinations. The test sample, composed of Compaq and HRID datasets, has 1000 images as the training set, while 2000 images are used for the test set. Both skin images and nonskin images were included. From the experimental results, it can be found that the recognition results of the same skin detection model in different color spaces exist for different recognized areas and share some uniform regions.

Sets $A$ and $B$ are the detection results in two color spaces, and the complementary (CPL) of the two color spaces are defined as follows: Complementary indicates the diversity between the two color spaces. The range of CPL is [0, 1]. CPL can be calculated from Eq. (4):

$$\mathrm{CPL} = \frac{(A_{\mathrm{TP}} \cup B_{\mathrm{TP}}) - (A_{\mathrm{FP}} \cap B_{\mathrm{FP}})}{T_{\mathrm{skin}}}, \tag{4}$$

where $A_{\mathrm{TP}}$ indicates the number of pixels that were detected as true positive (TP) pixels in one color space, while $B_{\mathrm{TP}}$ indicates the number of pixels that were detected as TP pixels in the other space. Furthermore, $A_{\mathrm{FP}}$ and $B_{\mathrm{FP}}$ serve as the number of pixels detected as false positive (FP) pixels, respectively. $T_{\mathrm{skin}}$ is the total amount of pixels in the image. The larger the CPL value is, the better the complementarity between the two color spaces is. Through the combination of recognition results from two color spaces, better performance was achieved. On the contrary, when the CPL value is smaller, this indicates that combining the recognition results of two color spaces will cause a slight improvement.

Table 1 shows the complementarity between each color space from which we can obtain a combination of RGB and HSV that works better, followed by the combination of RGB and YUV. These experimental data provide strong support for the use of a combination of multiple color spaces to improve the recognition effect.

#### 4.1.3. *Obtaining dual-threshold*

According to the statistical data of a large number of samples, the lower bound and upper bound were selected. The color distribution probabilities of the samples to be

Table 1. Complementary between each color spaces (Unit: %).

| Color Space | RGB | HSV | HSL | YCbCr | YUV | XYZ | LUV | Lab |
|---|---|---|---|---|---|---|---|---|
| RGB | 74.5 | 89.7 | 86.9 | 87.8 | 88.9 | 85.3 | 82.7 | 83.5 |
| HSV | | 70.6 | 78.0 | 88.3 | 87.1 | 77.5 | 80.1 | 79.1 |
| HSL | | | 69.9 | 85.4 | 85.3 | 77.5 | 81.4 | 76.3 |
| YCbCr | | | | 70.7 | 78.9 | 78.5 | 81.1 | 77.1 |
| YUV | | | | | 72.8 | 80.6 | 80.0 | 79.3 |
| XYZ | | | | | | 64.5 | 75.3 | 71.6 |
| LUV | | | | | | | 66.6 | 70.7 |
| Lab | | | | | | | | 65.0 |

measured were represented by the statistical samples. The approach is described as follows:

(1) Count the labeled skin pixels in the training set using the statistical histogram method. For each color, there is Eq. (5):

$$S(\text{color}) = \sum \text{color}_{\text{skin}}, \tag{5}$$

where $S(\text{color})$ represents the total number of colors in the sample set that are skin color. $\text{Color}_{\text{skin}}$ stands for the number of colors marked as skin in each image. Meanwhile, $\text{color}_{\text{nonskin}}$ stands for the number of colors is marked as nonskin in each image. In the same way, the frequency of each color that does not serve as a skin color can be acquired as Eq. (6):

$$N(\text{color}) = \sum \text{color}_{\text{nonskin}}. \tag{6}$$

The total number of skin pixels in the sample set is shown as Eq. (7):

$$T_s = \sum S(\text{color}). \tag{7}$$

The total number of the nonskin pixels in the sample set is shown as Eq. (8):

$$T_n = \sum N(\text{color}). \tag{8}$$

According to the Bayesian algorithm, $L(\text{color})$ are obtained for every color. For each color, the corresponding $L(\text{color})$, $S(\text{color})$ and $N(\text{color})$ are preserved.

(2) Sort $L(\text{color})$ values in descending order. The number of correctly detected skin pixels $C_s$ (Eq. (9)) and nonskin pixels $C_n$ (Eq. (10)) needed to attain the corresponding recognition rate and error rate are calculated based on the TPR and FPR selected.

$$C_s = \text{TPR} \cdot T_s, \tag{9}$$

$$C_n = \text{FPR} \cdot T_n. \tag{10}$$

(3) Accumulate the number of colors detected as skin $C_s'$ and nonskin $C_n'$, respectively. According to sorted $L(\text{color})$ and the dual-threshold ($\theta_1$ and $\theta_2$), they are recorded when the values are greater than or equal to $C_s$ and $C_n$, respectively. The larger number is treated as the upper bound, and the smaller numerical value is treated as the lower bound.

**Algorithm**: Dual-threshold Bayesian Algorithm
Input: TPR, FPR, Image sets
Output: Images with skin pixels labeled

FOR each color space
  Get $\theta_1[i]$ and $\theta_2[i]$ ($\theta_1[i] > \theta_2[i]$)
END FOR

IF $L_i(\text{color}) \geq \theta_1[i]$
  $G_i(x,y) = \text{Skin}$
ELSE IF $\theta_1[i] < L_i(color) < \theta_2[i]$
  $G_i(x,y) = \text{Undetermined}$
ELSE IF $L_i(\text{color}) \leq \theta_2[i]$
  $G_i(x,y) = \text{NonSkin}$
END IF

// $n_s$ is the number of color spaces labeled as skin
IF number of ($G_i(x,y) = \text{Skin}$ )$\geq n_s$
  $g(x,y) = \text{Skin}$
//$n_n$ is the number of color spaces labeled as non-skin
ELSE IF number of ($G_i(x,y) = \text{NonSkin}$) $\geq n_n$
  $g(x,y) = \text{NonSkin}$
ELSE
  $f_i(x,y) = L(color)$ *in color space i* ,
  $\alpha_i = \frac{Precision_i}{\sum_{i=0}^{n} Precision_i}$
//$M(color)$ indicates sum of multiple color spaces' value.
$M(color) = \alpha_1 f_1(x,y) + \alpha_2 f_2(x,y) + \cdots + \alpha_i f_i(x,y)$
  IF $M(color) \geq \theta_s$
    $g(x,y) = \text{Skin}$
  ELSE
    $g(x,y) = \text{NonSkin}$
  END IF
END IF

Fig. 2. Pseudocode of the DTBA.

As showed in Fig. 2, in the DTBA, the computation of each color space is independent as a consequence that parallel computing is feasible. Therefore, it can be extended to distributed systems.

### 4.2. *Skin texture characteristics and morphological filtering*

The approach above is not effective in identifying the pixels similar to the skin color, such as animal's fur, carpet, and desert, because only the color information was taken into account in the skin detection process. For the purpose of distinguishing the skin likely pixels better, skin texture characteristics were introduced to filter the recognition result. The texture features mean the relationship between the pixel and the

ambient pixels in gray space. Gray level co-occurrence matrix (GLCM) was proposed after analyzing the spatial dependency of the gray level.[12] The texture features of an image were well represented by the Gabor filter, which was considered as an adjustable edge detector in scale and direction. Skin texture has special characteristics in that the skin area appears in patches. Moreover, in gray color space, the differential between the skin pixels is small. Furthermore, the skin texture generally does not have textons, and the skin areas are irregular. Statistical analysis methods are suitable for extracting the features of skin texture. GLCM is a good choice. More specifically, $\overline{P}_\delta(i,j)$ indicates GLCM, where $(i,j=0,1,2,\ldots,L-1)$. It stands that the joint probability distribution of two pixels has grayscales that are $i$ and $j$. $L$ is the grayscale of the image. To illustrate, angular second moment (ASM), also known as energy, represents the smoothness and uniformity of the grey distribution of a region in the image. The expression for the field of view is Eq. (11)[12]:

$$\text{ASM:} f_1 = \sum_{i=0}^{L-1}\sum_{j=0}^{L-1} \overline{P}_\delta^2(i,j). \tag{11}$$

Contrast (CON) is used to measure the intensity of the differences between the surrounding pixels, which can reflect the clarity of the texture and can be expressed as Eq. (12)[12]:

$$\text{CON:} f_2 = \sum_{i=0}^{L-1}\sum_{j=0}^{L-1} (i-j)^2 \overline{P}_\delta(i,j). \tag{12}$$

Entropy (ENT) is the measurement of the information in an image. The value of ENT increased when the number of textures in the image increased. As shown in Eq. (13)[12]:

$$\text{ENT:} f_3 = \sum_{i=0}^{L-1}\sum_{j=0}^{L-1} \overline{P}_\delta(i,j) \cdot \log\left[\overline{P}_\delta(i,j)\right]. \tag{13}$$

Homogeneity (HOM) indicates the degree of uniformity in the texture distribution of the image and the change in the partial texture. As shown in Eq. (14)[34]:

$$\text{HOM:} f_4 = \sum_{i=0}^{L-1}\sum_{j=0}^{L-1} \frac{\overline{P}_\delta(i,j)}{1+(i-j)^2}. \tag{14}$$

On the basis of the texture features, we can construct a function using the features described above to determine whether a pixel belongs to skin. The first step of the skin texture feature filter is converting the image to grayscale. Then, using the 3×3 pixels as a unit, compute the GLCM of the image in the direction of 0°, 45°, 90°, and 135°, respectively. After that, calculate the ASM, CON, ENT, and HOM. Finally, a joint classifier is constructed using the weighted sum (F) of the four features as shown in Eq. (15):

$$\text{F} = \alpha_1 f_1 + \alpha_2 f_2 + \alpha_3 f_3 + \alpha_4 f_4 < \theta_{\text{skin}}, \tag{15}$$

where $\theta_{\text{skin}}$ is the classification threshold of skin texture features. The weight ($\alpha_i$) of each feature is the corresponding precision as shown in Eq. (16):

$$\alpha_i = \frac{\text{TP}_i}{\text{TP}_i + \text{FP}_i}, \tag{16}$$

where $\text{TP}_i$ stands for the total number of skin pixels detected correctly in color space $i$ and $\text{FP}_i$ stands for the total number of nonskin pixels detected as skin. The pixel will be marked as skin if the results are smaller than the threshold and vice versa. The skin texture filtering results are obtained after filtering the DTBA results with skin texture features.

The isolated noise and mistakenly recognized pixels occurred in the filtered skin areas with an unsmooth boundary through the processes above. These detection errors can be divided into two categories: one category is holes caused by error detection, and the other category is nonskin pixels incorrectly detected as skin. The errors are randomly distributed, and they can hardly be eliminated in regular ways. As a consequence, the morphological method was introduced to optimize the detection result. In morphological operations, structure element (SE) is the probe that is used to gather information. The structure information of the image is collected through the movement of the probe in the image. The difference in SE affects the operation results. Dilation and erosion are the bases of morphology. The opening operation is the process that erodes the image with the SE first and then dilates the results. The opening operation can smooth the object contour, disconnect the narrow neck, and eliminate pepper noise. In contrast, the closing operation is the process that dilates the image with the SE and erodes the results in sequence. It is efficient to smooth the outline of objects, connect narrow discontinuities, and eliminate holes. By using a circular SE to open and close the image in turn, the approach can reduce the detection error rate and improve the effect of skin detection.

## 5. Experiments and Discussion

In this section, we discuss and analyze the hybrid skin detection model we presented. Our model is compared with state-of-the-art skin detection models in the same test set and the same environment.

### 5.1. *Dataset*

The test sets of our model use the Compaq[a] image dataset and high-resolution image dataset (HRID)[b]. The Compaq dataset was collected in 1999. To explore the change in the images, we established a new dataset called HRID, which was obtained by

[a] The Compaq dataset is freely available for academic research purposes. Contact the author M. J. Jones (Michael.Jones@compaq.com) to obtain dataset.[3]

[b] The HRID dataset of labeled skin and nonskin pixels is freely available for academic research purposes. Contact the first author F. Chen (kuchen@csu.edu.cn) for instructions on how to obtain dataset.

Table 2. Statistical data of HRID.

| HRID | Total Pixels | Occupied Bins | Percent (%) | Images |
|---|---|---|---|---|
| All | 13,643,978,626 | 4,780,469 | 28.49 | 815 |
| Skin | 768,603,817 | 957,840 | 5.71 | 366 |
| Nonskin | 7,847,206,587 | 4,427,543 | 26.39 | 449 |

using a web crawler. Any images received from HRID whose resolution was less than 3000×2000 were excluded. In addition, the skin areas were labeled the same as the Compaq dataset. The statistical data from HRID is shown in Table 2. The bins stand for the quantity of per channel average allocated. For example, 32 bins in the RGB color space means that each R, G, and B channel was averagely divided into 32 parts.

HRID contains images of different people under a variety of illuminations from all types of perspectives. The total number of pixels is up to 7.6 billion. Because of the high resolution of the images, more details were contained in the images and a wider range of skin colors were covered. The images are closer to the human visual sense. At the same time, we modified the marks of skin pixels in Compaq to improve the recognition accuracy and precision (Fig. 3). As we can see from the images, themismarked pixels are eliminated while the missing skin pixels are added.

There are more than 13 times the number of pixels in HRID compared with Compaq. This means that more bins are occupied in skin than nonskin. Jones demonstrated the suitable bins for each channel. In the Compaq dataset, the skin detection model received the best results when each channel was divided into 32 bins. Because of the small number of bins for each channel, the detection model will obtain a high error rate, while having too many bins for each channel will lead to tremendous computation[6,13,14]. In this paper, we use the maximum amount of bins for each channel to obtain more accurate thresholds. In other phases, 32 bins is the default number of bins per channel.

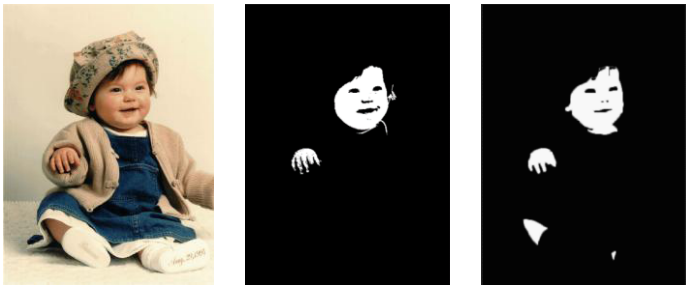

(a) (b) (c)

Fig. 3. Example of improvement in an image's mark in the Compaq. (a) initial image, (b) initial mark, and (c) modified mark.

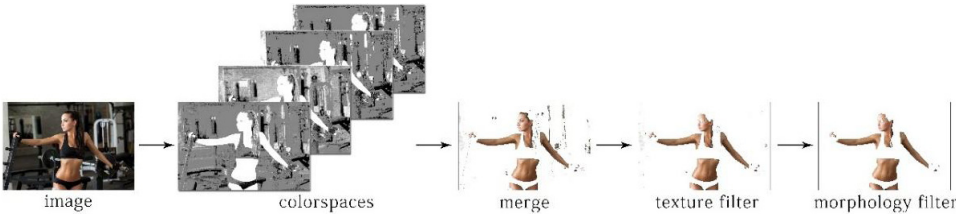


Fig. 4. The process of skin detection. First, the source image was detected in four color spaces using DTBA. Then, the merged skin area was obtained by combining the four results. Afterward, a texture filter was introduced followed by a morphology filter. Finally, the recognition result was acquired.

### 5.2. *Comparison and analysis*

We compared the hybrid skin detection model with other previous skin detection models in Compaq and HRID. The influence of each approach was taken into account. The processes of the skin detection model we presented are shown in Fig. 4. First, DTBA was used to classify skin pixels in each color space. Second, the detection results were merged into an image. Then, the combined image was filtered by skin texture and morphology, which became the final result.

#### 5.2.1. *DTBA based on multiple color spaces*

When DTBA is used to classify skin pixels in images, white indicates that the pixel is detected as skin, black indicates that the pixel is detected as nonskin, and grey means undetermined. The output images tend to be whitish mainly because of the high TPR set when obtaining all of the skin pixels. However, it causes a high error rate at the same time. Comparisons between naïve Bayesian and DTBA in a single color space and multiple color spaces are drawn in Fig. 5, which are tested on both Compaq and HRID datasets. We analyzed the performances of all models by using the receiver operating characteristic (ROC) curve. More specifically, the TPR and FPR are the criteria determined in the models. Moreover, every (FPR, TPR) rate was plotted on the coordinates where all of the points in the same model were connected by a smooth curve.

Where the white color stands for the pixel that is detected as skin, the black color indicates that the pixel was detected as nonskin and the gray color stands for the pixel that is detected as an undetermined pixel.

According to the ROC curves of the skin detection model, the following conclusions can be drawn from Fig. 6:

(1) In the same skin detection model, HRID acquired better outcomes. Because of the advanced image capture devices used in HRID, more realistic skin tones were obtained, which was beneficial for skin segmentation. Greater resolution also means more accurate details.

(2) The naïve Bayesian method based on multiple color spaces is superior to the naïve Bayesian method based on a single color space because information is used

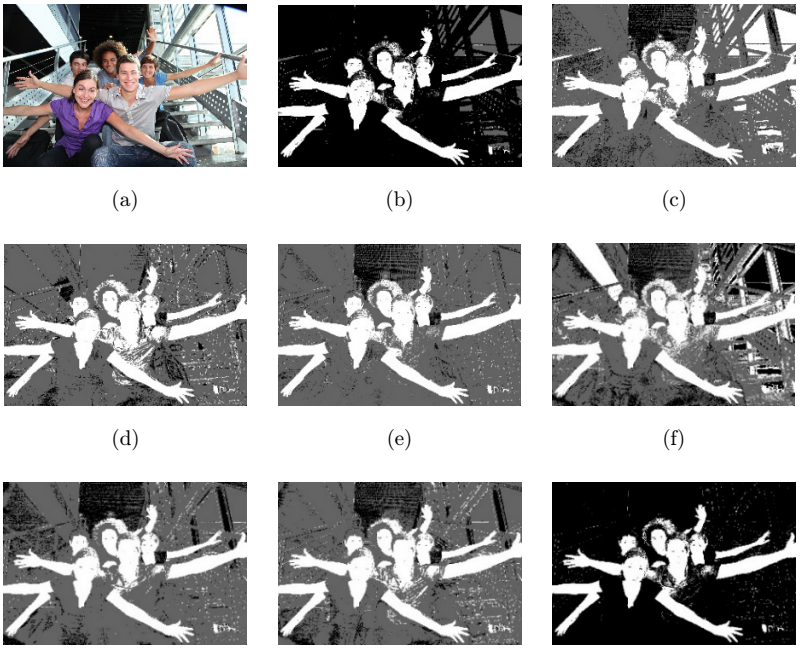


Fig. 5. Results of different color spaces using DTBA and the merged results. (a) initial image (b) HLS (c) HSV (d) LUV (e) RGB (f) XYZ (g) YCbCr (h) YUV (i) merged result from (b)–(h).

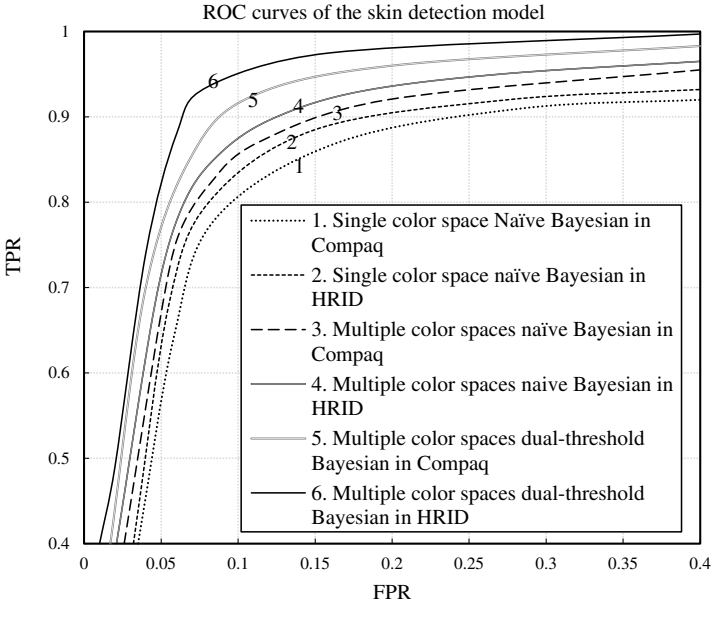


Fig. 6. The detection results using naïve Bayesian and DTBA in Compaq and HRID.

from various color spaces. This can make up for the deficiency of the single color space.

(3) The detection effect of DTBA is more precise than the naïve Bayesian method based on multiple color spaces. As described in Sec. 4, the pixels were classified into three categories. In the skin and nonskin categories, the correct detection rate goes up to 99%. Then, the following step concentrated on the undetermined pixels. Significant improvement is gained by allotting different weights to the detection results of each color space.

Moreover, we compared DTBA with the three threshold Bayesian algorithms based on multiple color spaces. A slight improvement was obtained, but the amount of computation increased. Other methods are needed to optimize the result by virtue of some of the overlaps between the skin and nonskin colors.

### 5.2.2. *Optimal quantity of color spaces*

We recorded the TPRs and FPRs of the detection results by testing each combination of color spaces. The number of color spaces determined the possible combinations of color spaces. The optimal results of the combinations, which were different in a number of color spaces, were compared (Fig. 7). As shown in Fig. 7, the recognition results turned out to be worst when the number of color spaces used was two. Moreover, no large difference occurred because the number of color spaces was greater than three. Owing to the excessive number of color spaces, this leads to a slight improvement in the detection results, whereas the computation has risen rapidly. As a consequence, we choose four color spaces as the best combination.

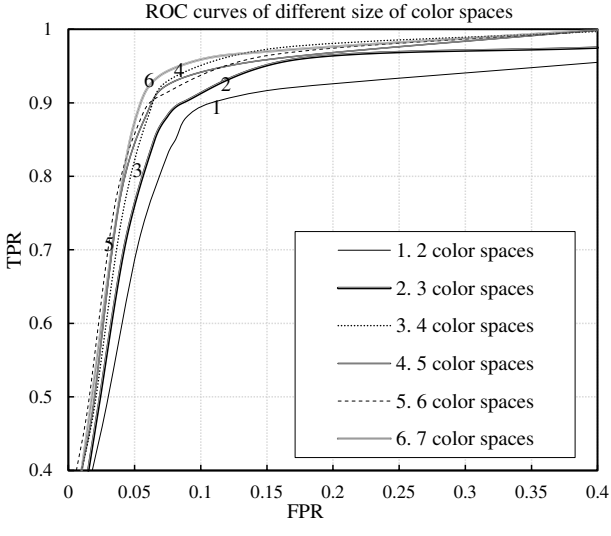


Fig. 7. ROC curves for different numbers of color spaces.

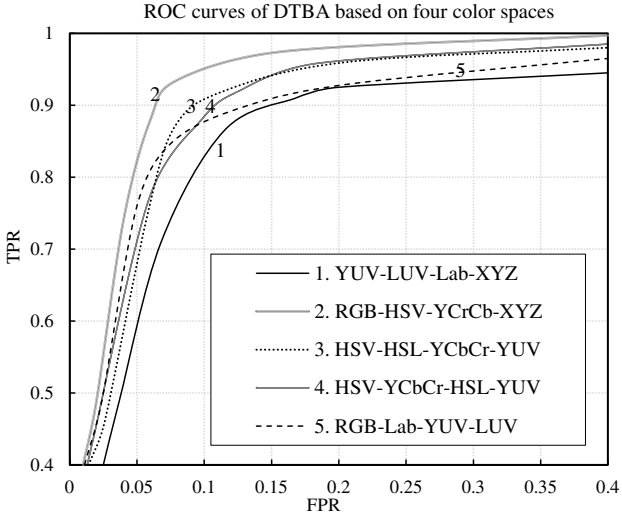


Fig. 8. ROC curves of the representative combinations for four color spaces using DTBA.

Further, the representative combinations of the four color spaces were compared (Fig. 8).

### 5.2.3. *Skin texture and morphological filtering*

At the previous phase, we utilized DTBA to classify skin pixels. To include the majority of the skin pixels, a high TPR was used to ensure it. However, a high error rate occurred in the meantime. Because of the inability of DTBA to distinguish the similar skin color, such as animal fur, sere grasses (Fig. 9) were mistakenly labeled.

In (b)–(d), the white color stands for the pixel that is detected as skin, the black color indicates the pixel that was detected as nonskin, and the gray color in (b) stands for the pixel that is detected as an undetermined pixel. Thus, additional steps will be taken.

Based on the results of DTBA, calculating the GLCM of pixels labeled as skin determines whether they are in accordance with the skin texture. Using the skin texture filter can make up for the disadvantages in the detection of similar skin color to achieve a lower error rate. As we can see from Fig. 10, the improvements are significant. By adding the weight value to texture features, the detection results were optimized.

The final step of the hybrid model is filtrating the results with the morphology filter. From the experimental results, executing the opening operation first and the closing operation second for the detection results worked best. The filter can effectively remove noise and can eliminate small holes and the smooth edge of.

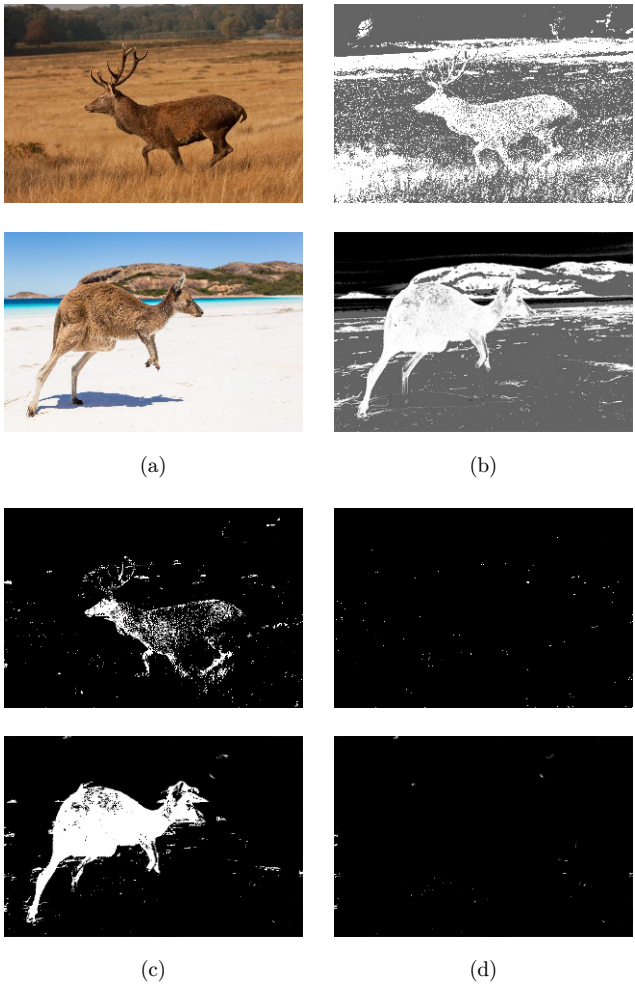

Fig. 9. Detection results of similar skin color. (a) Source image, (b) RGB using DTBA ($\text{threshold}_1 = 0.1$, $\text{threshold}_2 = 0.94$), (c) DTBA based on four color spaces, and (d) results of DTBA based on four color spaces used in skin texture filter.

### 5.2.4. *Comparison of skin detection models*

The hybrid skin detection model we presented in this paper executed multi-level filters. The model was verified in complex backgrounds. Five hundred images were used as the test set, and the outcomes are shown in Table 3. We can reach the conclusion that the model we proposed works well in complex backgrounds. Specifically, several examples are shown in Fig. 11. The images show that the Bayesian method can also recognize the skin in the glass reflection. More importantly, the hybrid skin model refined the results, especially in those situations where the image contains many people or has intricate surroundings.

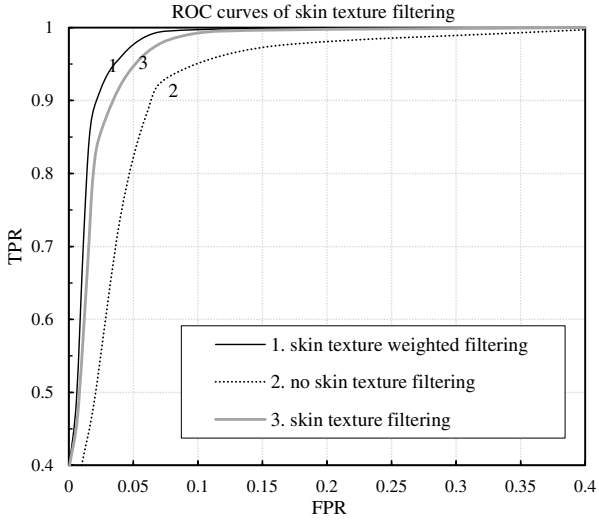


Fig. 10. ROC curves of skin texture filtering. Including skin texture weighted filter, skin texture filter, and no skin texture filter.

As shown in Table 3, compared with the naïve Bayesian algorithm, DTBA is based on multiple color spaces. The FPR is reduced by approximately 50%, namely, from 18.8% to 9.1%. More importantly, the hybrid skin model we proposed performed well under the complex environment, especially in HRID. It is up to 96.2% of the TPR with a distracted background. We compared the models in the Compaq and HRID datasets to show the advancement of the model we proposed (Table 4).

In the experiments, we used TPR (95%) and FPR (5%) as initial inputs to gain dual-thresholds. Experimentally, we found that the DTBA based on four color spaces was more precise and accurate than the Naïve Bayesian algorithm. To illustrate, the FPR of DTBA compared with the naïve Bayesian algorithm was reduced by 7.5% with a 2.6% increase in TPR. TPR is becoming more difficult to improve when it is more than 90%. The findings have demonstrated that the proposed approach produced TPRs of 95.5% and 97.4% in the Compaq dataset and in the HRID, respectively, and the FPRs are only 2.8% and 2.4%, respectively. Particularly, nearly one-third of the images received a TPR of more than 99%, which is

Table 3. Performance of models in complex background (unit: %)

| Models | Compaq TPR (FPR) | HRID TPR (FPR) |
|---|---|---|
| Naïve Bayesian[13] | 89.5(18.8) | 89.7(17.5) |
| Bayesian based on multiple color spaces | 90.0(16.2) | 91.2(15.8) |
| DTBA based on multiple color spaces | 92.8(9.1) | 93.3(8.8) |
| Gaussian mixture model[20] | 82.2(12.2) | 81.6(11.2) |
| Hybrid skin model (this paper) | 94.1(3.9) | 96.2(3.4) |

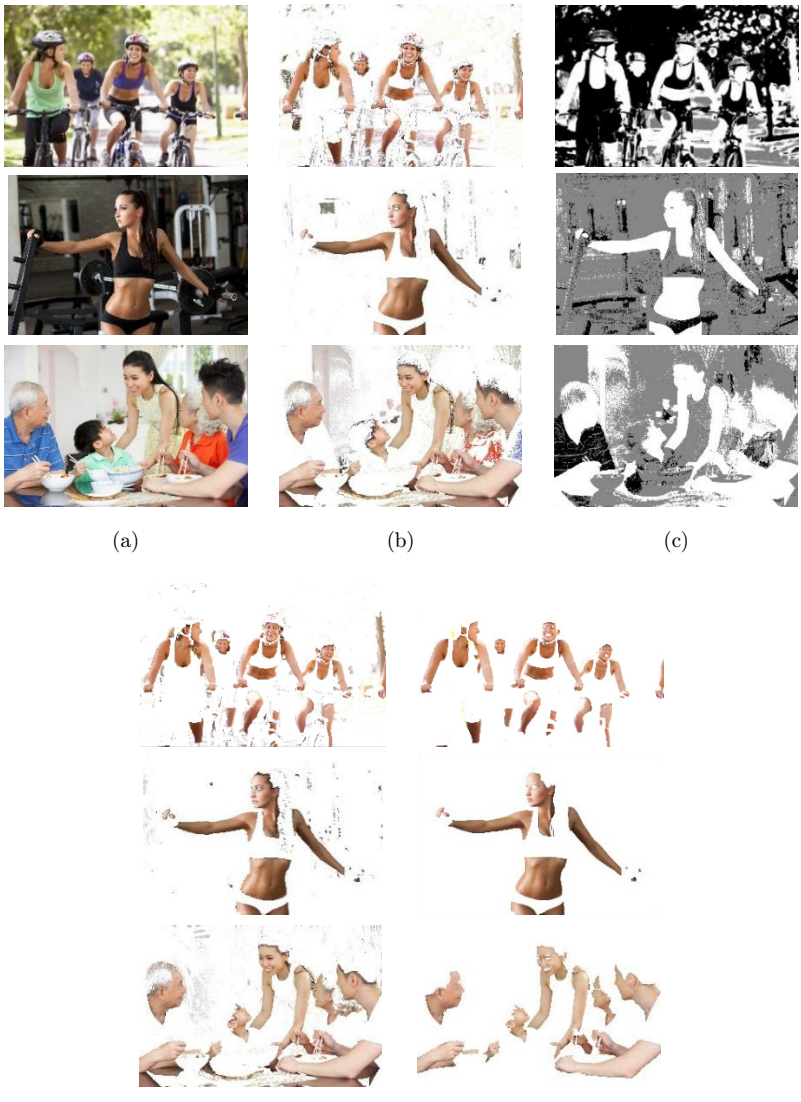

Fig. 11. Detection results in complex background. (a) initial image, (b) naïve Bayesian method (threshold = 0.71), (c) RGB using DTBA (threshold$_1$ = 0.1, threshold$_2$ = 0.93), (d) merged threshold result (threshold$_{skin}$ = 0.85) and (e) final result.

extremely precise. In order to improve the detection accuracy, plenty of models take advantage of other recognition methods, such as face, hand, and upper-body recognition.[5,10,15,21] Compare with those models, on the one hand, our hybrid model does not depend on face or hand in the image, on the other hand, our model needs less time to detect skin.

Table 4. Performance of models in two datasets (unit: %).

| Models | Compaq TPR (FPR) | HRID TPR (FPR) |
|---|---|---|
| Naïve Bayesian[13] | 90.5(14.8) | 91.2(13.6) |
| Bayesian based on multiple color spaces | 92.7(8.5) | 93.3(8.2) |
| DTBA based on multiple color spaces | 93.1(7.3) | 93.5(7.0) |
| Gaussian mixture model[20] | 85.4(10.1) | 86.2(9.6) |
| Hybrid skin model (this paper) | 95.5(2.8) | 97.4(2.4) |

Table 5. Performance of different skin detection.

| Models | Time(s) | TPR (%) | FPR (%) |
|---|---|---|---|
| Naïve Bayesian[13] | 0.0513 | 89.5 | 14.7 |
| Bayesian based on multiple color spaces | 0.1543 | 92.1 | 8.3 |
| DTBA based on multiple color spaces | 0.1986 | 92.5 | 7.5 |
| Gaussian mixture model[20] | 0.7428 | 87.2 | 9.1 |
| Skin texture Model[20] | 0.6863 | 88.5 | 14.3 |
| Hybrid skin model (this paper) | 0.3478 | 97.3 | 2.1 |

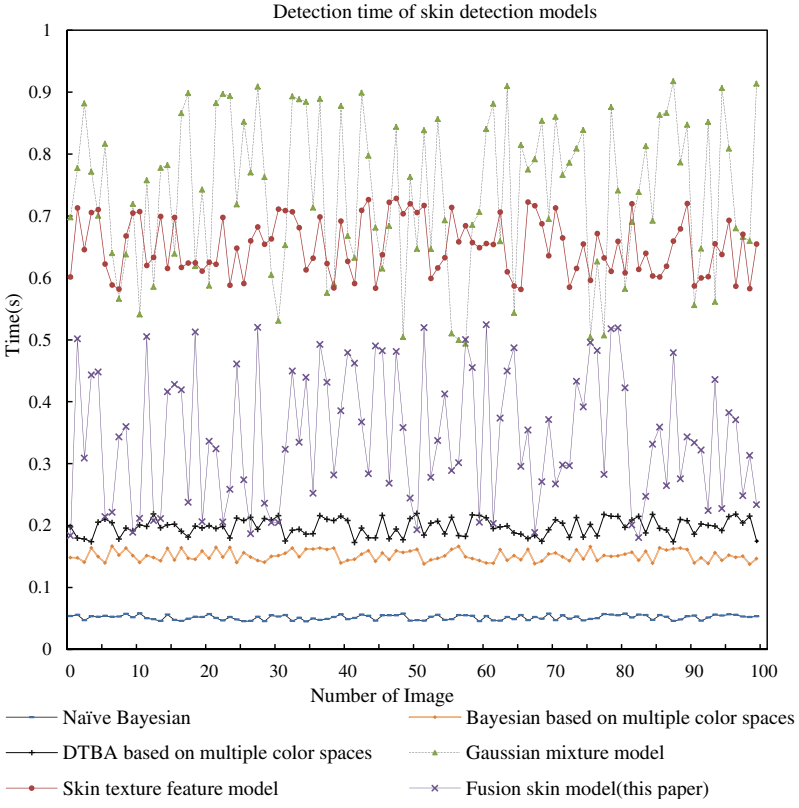


Fig. 12. Detection time of six skin detection models in each single image.

5.2.5. *Performance of skin detection*

To test the performance of the hybrid skin model we proposed, 150 images were taken in and each image had a resolution of 5120×2880. Among them, 50 images were used for the training set, while 100 images were used as the test set. The skin pixels occupied every image range from 10% to 70%. The experiment was finished in C++ in a PC with an 8 GB memory.

The average detection time of different skin models is shown in Table 5 along with TPR and FPR. The detection time of several models was compared on the test set (Fig. 12). From the diagram, we can draw the conclusion that the naïve Bayesian algorithm consumed the shortest amount of time and that this has nothing to do with the skin pixels contained in the images. On the contrary, the skin texture feature model requires massive computation. The hybrid skin detection model is superior to the former model, and the detection time is positively correlated to the number of skin pixels in the image.

Although the DTBA consumed more time than the naïve Bayesian algorithm, DTBA needs less computation time than the GMM and the skin texture model. Moreover, only the pixels detected as skin will be executed with skin texture filtering, whose computation was one-third as the skin texture model. Furthermore, the hybrid model acquired excellent TPRs and FPRs in an acceptable detection time. Compared with the neural network method, the hybrid model proposed in this paper does not require a complex construction process. The pictures we used in the test are more than 15 MB, however, a video taken by a real-time system usually less than 15M megabyte per second. For example, a 1080P (1920×1080) video, there are 1920 lines of horizontal pixels and 1080 lines of vertical pixels, taken by a camera, approximately 2 megabyte per second. So it can be applied in a real-time system. Sequential implementation of the proposed method allows for processing from 30 to 40 frames per second with the resolution of 1920×1080. In addition, the performance can be improved as the DTBA can be applied in the distributed system.

## 6. Conclusion

The development of hardware provides a perfect habitat for the software, and skin detection can make use of it. The DTBA we proposed took advantage of multiple color spaces and performed well in complex circumstances. First, the skin regions of Compaq were refined by us. In addition, HRID was presented and was more accurate in representing skin color and nonskin color. Second, DTBA was used as the first step for skin detection, and better detection results were obtained when it was combined with the skin texture feature filter. The hybrid skin detection model established in this paper classified the pixels with high accuracy and precision, and it is robust for a complex background. Finally, it can be applied in a real-time system. Because of the continuity and aggregation of skin areas, DTBA can be

applied in clustering classification. Through skin detection in every color space, we can set the pixel as a skin seed when it is true under strict conditions, such as a pixel detected as skin in all color spaces. In addition, a nonskin seed can be received when a pixel is detected as nonskin in all color spaces. Utilizing the approach described above, we can obtain two-way clustering, and there is no need to manually label the skin pixels. Incidentally, DTBA has general applicability and the potential for development in hair detection, gesture recognition, and object recognition.

## References


1. Y. Ban, S. K. Kim and S. Kim, Face detection based on skin color likelihood, *Pattern Recogn.* **47** (2014) 1573–1585.
2. M. A. Berbar, Novel colors correction approaches for natural scenes and skin detection techniques, *Int. J. Video and Image Process Netw. Secur. IJVIPNS-IJENS* **11**(2) (2011) 1–10.
3. K. K. Bhoyar and G. Kakde, Skin color detection model using neural networks and its performance evaluation, *J. Comput. Sci.* **6**(9) (2010) 963–968.
4. S. Bianco, F. Gasparini and R. Schettini, Adaptive skin classification using face and body detection, *IEEE Trans. Image Proces.* **24**(12) (2015) 4756–4765.
5. S. Bilal, R. Akmeliawati and M. J. E. Salami, Dynamic approach for real-time skin detection, *J. Real-Time Image Proces.* **10**(2) (2015) 371–385.
6. D. Chai and K. N. Ngan, Locating facial region of a head-and-shoulders color image, in *Proc. 3rd Int. Conf. Automatic Face and Gesture Recognition* (Nara, Japan, 1998), pp. 124–129.
7. Y. H. Chen and K. T. Hu, Statistical skin color detection method without color transformation for real-time surveillance systems, *Eng. Appl. Artif. Intell.* **25** (2012) 1331–1337.
8. C. A. Doukim and J. A. Dargham, Combining neural networks for skin detection, *Signal Image Proces.* **1**(2) (2010) 1129–1138.
9. L. Duan and Z. Lin, *Advances in Neural Networks*, A method of human skin region detection based on PCNN, Advances in Neural Networks, *6th International Symposium on Neural Networks, ISNN 2009, Proc, Part III* (Wuhan, China, 2009), pp. 486–493.
10. S. Duffner and J. M. Odobez, Leveraging colour segmentation for upper-body detection, *Pattern Recogn.* **47**(6) (2014) 2222–2230.
11. C. Garcia and G. Tziritas, Face detection using quantized skin color regions merging and wavelet packet analysis, *Trans. Multimed.* **1**(3) (1999) 264–277.
12. R. M. Haralick and K. Shanmugan, Textual features for image classification, *IEEE Trans. Syst. Man Cybern.* **3**(6) (1973) 610–621.
13. M. J. Jones and J. M. Rehg, Statistical color models with application to skin detection, *Int. J. Comput. Vis.* **46**(1) (2002) 81–96.
14. P. Kakumanu and S. Markrogiannis, A survey of skin-color modeling and detection methods, *Pattern Recogn.* **40** (2007) 1106–1122.
15. M. Kawulok, J. Kawulok and J. Nalepa, Skin detection using spatial analysis with adaptive seed, *Image Processing (ICIP), 2013 20th IEEE Int. Conf. IEEE* (Melbourne, Victoria, Australia, 2013), pp. 3720–3724.
16. M. Kawulok, J. Kawulok and J. Nalepa, Spatial-based skin detection using discriminative skin-presence features, *Pattern Recogn. Lett.* **41**(1) (2014) 3–13.

17. T. T. Khac, K. Q. Li and Y. Xu, Chemical reaction optimization with greedy strategy for the 0–1 knapsack problem, *Appli. Soft Comput.* **13**(4) (2013) 1774–1780.
18. S. A. Naji and R. Zainumddin, Skin segmentation based on multi pixel color clustering models, *Digit. Signal Process.* **22** (2012) 933–940.
19. P. P. Paul and M. Gavrillova, PCA based geometric modeling for automatic face detection, *Comput. Sci. Appl.* **4** (2011) 221–225.
20. H. Permuter, J. Francos and I. Jermyn, A study of gaussian mixture models of color and texture features for image classification and segmentation, *Pattern Recogn.* **39**(4) (2006) 695–706.
21. P. K. Pisharady, P. Vadakkepat and P. L. Ai, Attention based detection and recognition of hand postures against complex backgrounds, *Int. J. Comput. Vis.* **101**(3) (2013) 403–419.
22. J. C. SanMiguel and S. Suja, Skin detection by dual maximization of detectors agreement for video monitoring, *Pattern Recogn. Lett.* **34** (2013) 2102–2109.
23. M. Shoyaib and M. Abdullah-AI-Wadud, A skin detection approach based on the Dempster-Shafer theory of evidence, *Int. J. Approx. Reason.* **53** (2012) 636–659.
24. M. C. Skin and K. I. Chang, Does colorspace transformation make any difference on skin detection, in *Proc. IEEE Workshop on Applications of Computer Vision.* (Orlando, FL, USA, 2002) 275–279.
25. F. Y. Song, X. Y. Tan and L. Xue, Eyes closeness detection from still images with multi-scale histograms of principal oriented gradients, *Pattern Recogn.* **47** (2014) 2825–2838.
26. H. M. Sun, Skin detection for single images using dynamic skin color modeling, *Pattern Recogn.* **43** (2010) 1413–1420.
27. J. Terrillon and S. Akamatsu, Comparative performance of different chrominance spaces for color segmentation and detection of human faces in complex scene images, *Vis. Interf.* **99** (1999) 180–187.
28. A. Tsitsoulis, G. Nikolaos and Bourbakis, A methodology for extracting standing human bodies from single images, *Trans. Hum.–Mach. Syst.* **45**(3) (2015) 327–338.
29. M. A. Wadud and M. Shoyaib, A skin detection approach based on color distance map, *EURASIP J. Adv. Signal Process.* **10** (2008) 1–10.
30. F. Y. Xie and A. C. Bovik, Automatic segmentation of dermoscopy images using self-generating neural networks seeded by genetic algorithm, *Pattern Recogn.* **46** (2013) 1012–1019.
31. Y. Xu and K.Q. Li, A DAG scheduling scheme on heterogeneous computing systems using double molecular structure-based chemical reaction optimization, *J. Parallel Distrib. Comput.* **73**(9) (2013) 1306–1322.
32. P. Yogarajah, J. Condell and K. Curran, A dynamic threshold approach for skin segmentation in color images, *Int. J. Biometrics.* **4**(5) (2012) 38–55.
33. A. A. Zaidan and N. N. Ahmad, Image skin segmentation based on multi-agent learning Bayesian and neural network, *Eng. Appl. Artif. Intell.* **32** (2014) 136–150.
34. A. A. Zaidan, H. A. Karim and N. N. Ahmad, An automated anti-pornography system using a skin detector based on artificial intelligence: A review, *Int. J. Pattern Recogn. Artif. Intell.* **27**(4)(2013) 254–261.
35. A. A. Zaidan, H. A. Karim and N. N. Ahmad, A four-phases methodology to propose anti-pornography system based on neural and Bayesian methods of artificial intelligence, *Int. J. Pattern Recogn. Artif. Intell.* **28**(1) (2014) 178–215.

**Fujunku Chen**, born in 1990, received his B.S degree in Software Engineering from Central South University, Changsha, China in 2013. He is currently studying in the Central South University as an undergraduate student of software engineering. He is committed to skin detection and image beautification. His research interests include software engineering, data mining and computer vision. In addition, he has participated in more than 10 software projects.

**Zhigang Hu**, born in 1963, is a Professor and Ph.D. supervisor of the Central South University, Changsha, China. He is also a senior member of China Computer Federation. He received his B.S. and his M.S. degrees from Central South University, Changsha, China in 1985 and in 1988, respectively. He received his Ph.D. from Central South University, Changsha, China in 2002. His research interests focus on the parallel computing, cloud computing and high performance computing. He has published many papers in international journals and conferences. He is the deputy Secretary-General of Hunan Computer Federation. He is currently the vice-dean of School of Software, Central South University.

**Keqin Li** is a SUNY Distinguished Professor of Computer Science. His current research interests include parallel computing and high-performance computing, distributed computing, energy-efficient computing and communication, heterogeneous computing systems, cloud computing, big data computing, CPU-GPU hybrid and cooperative computing, multicore computing, storage and file systems, wireless communication networks, sensor networks, peer-to-peer file sharing systems, mobile computing, service computing, Internet of things and cyber-physical systems. He has published over 400 journal articles, book chapters, and refereed conference papers, and has received several best paper awards. He is currently, or has served, on the editorial boards of IEEE Transactions on Parallel and Distributed Systems, IEEE Transactions on Computers, IEEE Transactions on Cloud Computing, Journal of Parallel and Distributed Computing. He is also an IEEE Fellow.

**Wei Liu**, born in 1982, is a member of China Computer Federation. He received his Ph.D. and his M.S. degree from Central South University, Changsha, China. His research interests focus on the software engineering and data mining, design patterns, and source code analysis and optimize. He has published more than 10 journal articles. Additionally, he has taken part in over 30 software projects.